NASA TECHNICAL NOTE

NASA TN D-3442

LOW-SUBSONIC WIND-TUNNEL AND FREE-FLIGHT DROP-TEST INVESTIGATION OF A PARAGLIDER CONFIGURATION HAVING LARGE TAPERED LEADING EDGES AND KEEL

by Delwin R. Croom and Paul G. Fournier

Langley Research Center
Langley Station, Hampton, Va.

NATIONAL AERONAUTICS AND SPACE ADMINISTRATION • WASHINGTON, D. C. • OCTOBER 1966

LOW-SUBSONIC WIND-TUNNEL AND FREE-FLIGHT DROP-TEST INVESTIGATION OF A PARAGLIDER CONFIGURATION HAVING LARGE TAPERED LEADING EDGES AND KEEL

By Delwin R. Croom and Paul G. Fournier

Langley Research Center
Langley Station, Hampton, Va.

Technical Film Supplement L-906 available on request.

NATIONAL AERONAUTICS AND SPACE ADMINISTRATION

For sale by the Clearinghouse for Federal Scientific and Technical Information
Springfield, Virginia 22151 – Price $2.00

LOW-SUBSONIC WIND-TUNNEL AND FREE-FLIGHT DROP-TEST INVESTIGATION OF A PARAGLIDER CONFIGURATION HAVING LARGE TAPERED LEADING EDGES AND KEEL

By Delwin R. Croom and Paul G. Fournier
Langley Research Center

SUMMARY

Low-subsonic wind-tunnel and free-flight drop-test investigations were made to evaluate the performance, stability, and free-flight characteristics of a paraglider configuration having large inflatable tapered leading edges and keel. Results obtained from the wind-tunnel tests indicated that the configuration had a maximum lift-drag ratio of approximately 3.0 and positive static longitudinal and lateral stability. The flight tests demonstrated that the configuration could be trimmed for steady gliding flight and was capable of recovering from launches at zero speed at extreme pitch attitudes and roll attitude.

INTRODUCTION

The paraglider has been considered by the Langley Research Center as a recovery device for expended booster rockets, manned spacecraft, and instrument payloads from orbital and suborbital flights. Experimental and analytical investigations have been made to evaluate the capabilities of the paraglider as a recovery device; some of the results of these studies have been reported in references 1 to 8.

The present paraglider configuration was designed to investigate micrometeoroid impacts in space by using an instrumented flexible canopy which provided a relatively large sensor area that could be recovered after reentry. The paraglider was of inflated-tube construction to allow packaging in the launch vehicle and deployment in space. Static force tests to determine the aerodynamic characteristics of a 0.0472-scale model of the configuration were made at Mach number 4.5 for angles of attack from 0^{o} to 360^{o} and sideslip angles from 0^{o} to 90^{o}. These supersonic results are presented in reference 5.

The present investigations were made to determine the low-speed static aerodynamic characteristics and flight behavior of the paraglider configuration. Static aerodynamic characteristics were obtained on both a 1/5-scale and a full-scale model; free-flight tests were made by an outdoor drop and uncontrolled glide technique with the full-scale model

used in the tunnel tests. A motion-picture supplement has been prepared of the flight tests and is available on loan. A request card and a description of the flim are included at the back of this paper.

SYMBOLS

The data presented in this report are referred to the axis system shown in figure 1. The moment reference for the data obtained on the 1/5-scale wing-alone configuration was located at 50 percent of the keel length and on the center line of the keel. The moment reference for the complete configurations was located below the wing as shown in figures 2 and 3.

The units used for the physical quantities in this paper are given both in the International System of Units (SI) and in the U.S. Customary Units. Details concerning the use of SI, together with physical constants and conversion factors, are given in reference 9.

b wing span, centimeters (inches) (see figs. 2 and 3)

C_A axial-force coefficient, $\frac{\text{Axial force}}{qS}$

C_D drag coefficient, $\frac{\text{Drag}}{qS}$

C_L lift coefficient, $\frac{\text{Lift}}{qS}$

C_l rolling-moment coefficient, $\frac{\text{Rolling moment}}{qSb}$

C_{l_β} effective dihedral parameter, $\left(\frac{\Delta C_l}{\Delta \beta}\right)_{\beta=\pm 5^o}$, per degree

C_m pitching-moment coefficient, $\frac{\text{Pitching moment}}{qSl_k}$

C_{m_α} longitudinal stability parameter, $\frac{\partial C_m}{\partial \alpha_k}$, per degree

C_N normal-force coefficient, $\frac{\text{Normal force}}{qS}$

C_n yawing-moment coefficient, $\frac{\text{Yawing moment}}{qSb}$

C_{n_β} directional stability parameter, $\left(\frac{\Delta C_n}{\Delta \beta}\right)_{\beta=\pm 5^o}$, per degree

C_T cable-tension coefficient, $\frac{\text{Cable tension}}{qS}$

C_Y side-force coefficient, $\frac{\text{Side force}}{qS}$

C_{Y_β} side-force parameter, $\left(\frac{\Delta C_Y}{\Delta \beta}\right)_{\beta=\pm 5^o}$, per degree

L/D lift-drag ratio, $\frac{C_L}{C_D}$

l_k length of wing keel from apex at intersection of leading-edge center lines to rear end of constant taper of keel, centimeters (inches) (see figs. 2 and 3)

l_{le} length of leading edge, measured from intersection of leading-edge center lines to tip of constant taper of leading edge, centimeters (inches)

q free-stream dynamic pressure, newtons/meter^2 (pounds/foot^2)

S flat planform area of wing canopy (to center line of leading edge), meters^2 (feet^2) (see figs. 2 and 3)

X,Y,Z longitudinal, lateral, and vertical body axis, respectively

x,z distance measured along X- and Z-axis, respectively

x_{cg} distance to center of gravity from wing apex, measured parallel to wing keel center line, centimeters (inches)

x_{cp} longitudinal position of center of pressure, expressed in terms of keel length, $0.50 - C_m/C_N$

z_{cg} distance to center of gravity below wing keel, measured perpendicular to keel center line in plane of symmetry, centimeters (inches)

α_k angle of attack of wing keel center line, degrees

β angle of sideslip, degrees

Λ leading-edge sweep angle, degrees

Subscripts:

o flat-planform condition

trim trimmed value

DESCRIPTION OF MODELS

1/5-Scale Model

The general arrangement of the 1/5-scale model is shown in figure 2. Pertinent geometric characteristics are presented in table I. A photograph of the 1/5-scale model in the Langley high-speed 7- by 10-foot tunnel is shown as figure 4. The simulated instrument package was made of aluminum and was attached to a six-component strain-gage balance mounted on a sting support. The structural members of the 1/5-scale model wing were made of soft balsa and were hollow except near the apex and cable attachment points. The leading edges and keel were reinforced with mahogany blocks at each cable attachment point, at the apex, and at the juncture with the spreader bar. In order to represent the shape of the inflatable parawing configuration, the wing leading edges and keel were tapered and had a relatively large diameter (maximum diameter of 11.9 percent of keel length, minimum diameter of 4.8 percent of keel length, see fig. 2). The wing leading edges were hinged at the apex and at the juncture of the spreader bar and keel as shown in figure 2, in order to measure the cable tensions in such a manner that the results would be applicable to an inflated-tube structure which furnished little or no moment restraint at these points. The wing canopy was made of stabilized dacron sail cloth weighing 166 g/m^2 (4.9 oz/yd^2). The canopy fabric weave was oriented with the warp running parallel to the trailing edge. The canopy was attached to the keel by a narrow aluminum strip 0.95 cm (3/8 in.) wide and 0.16 cm (1/16 in.) thick along the top of the keel and was attached to the leading edges by wrapping the canopy around the outside of the leading edges as shown in figure 2.

The wing was attached to the simulated instrument package by a relatively large tubular member (diameter of 7.14 percent of the keel length) to simulate an inflatable member and four 0.08-cm (1/32-in.) diameter stranded steel cables. Tension gages were installed in each cable just above the simulated instrument package. Standard fishing-line swivels were installed above and below each tension gage. All hooks and swivels were preloaded before installation on the model in order to check their strength and to eliminate changes in length due to loading during the tests.

Full-Scale Model

The general arrangement of the full-scale model is shown in figure 3. Pertinent geometric characteristics are presented in table I. A photograph of the model under test in the Langley full-scale tunnel is shown as figure 5. The frame of the model (leading edges, keel, nose section, and vertical tube) consisted of inflatable members that were made from a neoprene-coated nylon-twill fabric that weighed 170 g/m^2 (5 oz/yd^2). An aluminum sheath was fitted around the vertical tube and cradled a portion of the keel. The lower part of the sheath was bolted to the simulated instrument payload, which was a hollow aluminum pressure vessel. The sheath was attached to a strut-mounted six-component strain-gage balance.

The wing canopy was made of 166 g/m^2 (4.9 oz/yd^2) dacron sail cloth that had laminated to its upper surface an aluminum mylar sandwich material that was 0.1 mm (4 mils) in thickness to simulate the condenser material to be used in the proposed full-scale micrometeoroid experiment. The canopy fabric weave was oriented with the warp running parallel to the trailing edge. The canopy was attached to the keel and leading edges as shown in figure 3.

The wing was attached to the simulated instrument package by the inflated vertical tube which was inside the sheath and by four 0.32-cm (1/8-in.) diameter nylon cables. These cables stretched under air load and were later replaced by 0.32-cm-diameter steel cables as the tests proceeded; first the keel cables were replaced, then the leading-edge cables were replaced.

Prior to the full-scale wind-tunnel tests, the model was free-flown to observe the free-flight behavior of the configuration. During the flight program, only the nylon cables were used.

TESTS AND CORRECTIONS

Wind-Tunnel Tests of 1/5-Scale Model

The investigation of the 1/5-scale model was made in the Langley high-speed 7- by 10-foot tunnel. Longitudinal aerodynamic data were obtained of the wing-alone configuration at dynamic pressures of 478.8 and 574.6 N/m^2 (10 and 12 lb/ft^2) and for the complete configuration at a dynamic pressure of 574.6 N/m^2 through an angle-of-attack range from about 20^o to 50^o. Tension in the support cables between the wing and simulated instrument package was measured at dynamic pressures of 478.8 and 574.6 N/m^2 through an angle-of-attack range from about 21^o to 50^o and also at selected angles of attack between 22^o to 50^o through a dynamic-pressure range from 191.5 to 574.6 N/m^2 (4 to 12 lb/ft^2). Reynolds numbers for these test conditions, based on keel length, varied from about 1.0×10^6 (for $q = 191.5$ N/m^2) to about 1.6×10^6 (for $q = 574.6$ N/m^2).

Forces and moments were measured by means of a six-component strain-gage balance attached to the simulated instrument package for the complete configuration and to the underside of the keel for the wing-alone configuration and, in turn, attached to the variable angle sting-support system which was remotely controlled over an angle-of-attack range of approximately 24°. The angle-of-attack range could be extended by inserting an angle coupling in the main sting.

Angles of attack and sideslip have been corrected for effects of deflection of the sting and balance under aerodynamic load. No blockage corrections to dynamic pressure or jet-boundary corrections to angle of attack or drag coefficient have been applied to the data inasmuch as these corrections have been found to be small for models of this size in the perforated-slot configuration of the Langley high-speed 7- by 10-foot tunnel. No corrections have been made for sting-support tares inasmuch as the tare effects were not evaluated and are believed to be small.

Wind-Tunnel Tests of Full-Scale Model

The investigation of the full-scale model was made in the Langley full-scale tunnel at angles of attack ranging from about 20° to 55° and at sideslip angles of 0° and $\pm 5^{\circ}$. The range of dynamic pressure for these tests was from about 81.4 N/m^2 (1.7 lb/ft^2) to 205.9 N/m^2 (4.3 lb/ft^2). Reynolds numbers for these test conditions, based on the keel length, varied from about 3.5×10^6 (for $q = 81.4$ N/m^2) to about 5.4×10^6 (for $q = 205.9$ N/m^2). Force and moment measurements were made with a six-component strain-gage balance.

Jet-boundary corrections to angle of attack and drag have been made. No corrections have been made for sting-support tares or blockage effect inasmuch as these corrections are believed to be small.

Free-Flight Drop Tests of Full-Scale Model

The flight-test portion of the investigation consisted of a series of flights of the full-scale model to determine qualitatively the effect of longitudinal shift in center-of-gravity position on the free-flight stability and to determine by observation the vehicle's capability of recovering from pitch attitudes of about 90°, -90°, and 180° and from a roll attitude of about 90°. The free-flight stability tests were made with the model having wing loadings of 28.7 and 57.5 N/m^2 (0.6 and 1.2 lb/ft^2). The unusual-attitude recovery tests were made with the model having a wing loading of 28.7 N/m^2. The vertical center of gravity was located at approximately 45 percent of the keel length below the keel center line for all tests. The horizontal locations of the center of gravity were at 60, 65, and 70 percent of the keel length for the normal free-flight stability tests and at 65 percent of the keel length for the unusual-attitude recovery tests.

A helicopter equipped with a 91.4-m (300-ft) steel cable and an electrically operated release hook was used for these tests. For the normal free-flight stability tests, the model was released in forward flight and, for the unusual-attitude recovery tests, the model was released at an airspeed of zero.

Evaluation of the flight characteristics was based solely on the opinion of the observers. No quantitative data were obtained because of the exploratory nature of the test program. The qualitative data obtained consisted of motion-picture records of the flights taken with cameras located on the ground and in chase helicopters.

PRESENTATION OF RESULTS

The static longitudinal aerodynamic characteristics of the 1/5-scale wing-alone model and complete-model configurations are presented in figures 6 and 7, respectively. The cable-tension coefficients obtained on the 1/5-scale model are presented in figures 8 and 9 as a function of α_k and q, respectively. The static longitudinal aerodynamic characteristics of the full-scale model are presented in figures 10 and 11. The static lateral aerodynamic characteristics of the full-scale model are presented in figure 12.

The full-scale-model data (fig. 10, $q = 167.6$ N/m^2 (3.5 lb/ft^2)) were analyzed by using the method suggested in reference 10 and are presented in figure 13 to show the effect of center-of-gravity location on the trimmed-lift coefficient and static longitudinal stability. Motion-picture records of the free-flight drop tests of the full-scale model are available on request.

RESULTS AND DISCUSSION

Wind-Tunnel Tests

Longitudinal aerodynamic characteristics.- The aerodynamic characteristics presented in figure 6 for the 1/5-scale wing-alone configuration indicate that the maximum lift-drag ratio was about 3.5. This value of maximum lift-drag ratio compares favorably with the value of 3.3 obtained for the $\Lambda_o = 45^o$, $\Lambda = 55^o$ canopy-shape configuration and presented in figure 12 of reference 11 for a constant-diameter tube model. Test results presented in figure 7 for the 1/5-scale complete model configuration show that addition of the simulated instrument package, keel rigging lines, and vertical tube reduced the maximum lift-drag ratio to a value of 2.7.

Aerodynamic characteristics of the full-scale configuration, presented in figures 10 and 11, indicate that the maximum lift-drag ratio of the inflated-tube model varied slightly with test dynamic pressure and also varied with the type of support cables used between the wing and instrument package. The highest value of maximum lift-drag ratio

of 3.4 obtained on the full-scale model occurred at the lowest test dynamic pressure and with steel cables on the keel and nylon cables on the leading edges (fig. 10). During preliminary tests of the full-scale model with all lines nylon, the nose of the model was observed to deflect upward under air load. This deflection, caused by stretch of the nylon line at the nose, was so large that it was considered necessary to replace the nylon lines on the keel with steel cables. No test data were obtained with nylon lines on the keel because of the excessive keel deflection. Also observed was that increasing the test dynamic pressure q from 86.2 N/m^2 (1.8 lb/ft^2) to 167.6 N/m^2 (3.5 lb/ft^2) caused a large upward deflection of the leading edges, and this deflection caused the maximum lift-drag ratio to decrease from 3.4 to 3.15. The deflection of the leading edge appears to arise from both stretch in the nylon lines and the aeroelastic deflection of the leading edge itself. When the nylon lines to the leading edge were used, the deflections appeared to be distributed along the leading edge in a manner that provided a gradual reduction in wing twist across the span. Replacing the nylon lines with steel cables to the leading edge caused a noticeable localized upward deflection of the leading edge aft of the cables. Use of the steel cables on the leading edge caused the maximum lift-drag ratio at $q = 167.6$ N/m^2 to decrease to a value of about 3.1.

Comparison of maximum lift-drag ratios obtained from the 1/5-scale model and the full-scale model indicates that the full-scale model had somewhat higher lift-drag ratios. Reasons for this difference in lift-drag ratios are believed to be associated with the following factors. The use of a spreader bar on the 1/5-scale model contributed a drag increment which was not present for the full-scale model. In addition to the spreader bar, other construction details such as the nose shape (see figs. 2 and 3) and elasticity of the full-scale wing had an effect on the aerodynamic characteristics obtained on the two models. The pitching-moment data also indicated some difference in stability and trim for the two models in that the full-scale model had a slightly higher level of static stability and trimmed at a slightly higher lift coefficient than the 1/5-scale model.

Lateral aerodynamic characteristics.- The full-scale model was directionally stable throughout the test angle-of-attack range, and the magnitude of the directional stability parameter C_{n_β} increased with an increase in angle of attack. The model had positive effective dihedral $-C_{l_\beta}$ throughout the test angle-of-attack range and the magnitude of $-C_{l_\beta}$ increased with an increase in angle of attack. (See fig. 12.)

Cable-Tension Measurements

Measurements of leading-edge cable tension were made on the 1/5-scale model which had hinged leading edges and simulated a wing having no apex moment restraints about the hinge axis. (See fig. 2.) The comparison of cable-tension data and internal strain-gage balance data presented in reference 7 indicated that fairly reliable cable-tension data could be obtained for a hinged-tube model similar to the present 1/5-scale

model. The results of reference 7 also indicated that, for angles of attack below the design trim angle, the highest cable tension occurred in the two leading-edge cables; approximately one-half of the total load was carried in the leading-edge cables. For the present investigation, therefore, attention was given primarily to measurement of the tension in the leading-edge cables. Measurements of tension in the front and rear keel cables were made; however, the results obtained have little application to an inflated-tube design because of the moment restraint of the vertical tube at the keel.

The cable-tension coefficients for the leading-edge cables (fig. 8) for dynamic pressures of 478.8 and 574.6 N/m^2 (10 and 12 lb/ft^2) show the expected increase with increasing angle of attack. The maximum value of tension coefficient of about 0.3 was approximately the same as the maximum value obtained on the leading-edge lines in the results of reference 7. The test data obtained at $q = 478.8$ N/m^2 and 574.6 N/m^2 (fig. 8) were in very good agreement throughout the test angle-of-attack range. Test results over a range of dynamic pressures at constant angles of attack (fig. 9) showed only small variations in tension coefficient with test dynamic pressure; with the exception of the highest angles of attack, these variations occurred primarily below $q = 383.0$ N/m^2 (8 lb/ft^2).

Free-Flight Drop Tests

A preliminary weight estimate of the paraglider configuration designed to investigate meteoroid impacts indicated that the vehicle would have a wing loading of about 28.7 N/m^2 (0.6 lb/ft^2). However, because of the weight of material required to withstand heat and loads of reentry, the fabrication techniques used, the increased weight of paraglider inflation system, and the added onboard electronic equipment, the final vehicle wing loading was approximately 57.5 N/m^2 (1.2 lb/ft^2). The initial flights were made with a wing loading of 28.7 N/m^2 and later flights were made with a wing loading of 57.5 N/m^2. These tests were made to determine qualitatively the effects of longitudinal center-of-gravity location on the free-flight stability and also to observe the ability of the vehicle to recover from unusual attitudes. The unusual-attitude recovery tests were made for the wing loading of 28.7 N/m^2 only.

When the center of gravity was located longitudinally at 65 percent of the keel length, the model flew with no observable longitudinal or lateral oscillation, and the canopy was steady. The trimmed-lift coefficient for this flight condition, based on analysis of static full-scale wind-tunnel data, was about 0.76. (See fig. 13.) When the center of gravity was moved forward to the 60-percent-keel position $\left(C_{L,trim} \approx 0.54\right)$, the flight speed was increased and the canopy was somewhat unsteady and appeared to be approaching the luffing condition. When the center of gravity was located at the 70-percent-keel position $\left(C_{L,trim} \approx 1.02\right)$, the model flew with a slight phugoid oscillation. Based on the observed flight behavior, this particular configuration should be flown with the longitudinal center

of gravity near the 65-percent-keel location in order to obtain a steady glide. The unusual-attitude recovery tests were therefore made with the center of gravity at the 65-percent-keel position. The initial condition established for these tests was that the helicopter hover at zero airspeed and release the model at pitch attitudes of about 90^{o}, -90^{o}, and 180^{o} and also with the model rolled about 90^{o}. Even though very large angle-of-attack and sideslip excursions occurred in these tests, the motions were heavily damped, the model recovered quickly, sought its trim point, and established a steady glide.

SUMMARY OF RESULTS

The low-speed wind-tunnel test results obtained on a large inflated-tube paraglider indicated a maximum lift-drag ratio of approximately 3.0 and positive longitudinal stability throughout the test angle-of-attack range. The static directional stability and effective dihedral were positive through the test angle-of-attack range. Analysis of the wind-tunnel results indicated that the configuration could be trimmed over the entire lift-coefficient range by longitudinal shift of the center of gravity.

The flight tests indicated that the model could be trimmed for steady glide and was capable of recovering from initial drop conditions of extreme pitch attitudes and roll attitude.

Langley Research Center,
National Aeronautics and Space Administration,
Langley Station, Hampton, Va., April 26, 1966.

REFERENCES

1. Rogallo, Francis M.; Lowry, John G.; Croom, Delwin R.; and Taylor, Robert T.: Preliminary Investigation of a Paraglider. NASA TN D-443, 1960.

2. Taylor, Robert T.: Wind-Tunnel Investigation of Paraglider Models at Supersonic Speeds. NASA TN D-985, 1961.

3. Hatch, Howard G., Jr.; and McGowan, William A.: An Analytical Investigation of the Loads, Temperatures, and Ranges Obtained During the Recovery of Rocket Boosters by Means of a Parawing. NASA TN D-1003, 1962.

4. Penland, Jim A.: A Study of the Aerodynamic Characteristics of a Fixed Geometry Paraglider Configuration and Three Canopies With Simulated Variable Canopy Inflation at a Mach Number of 6.6. NASA TN D-1022, 1962.

5. Wornom, Dewey E.; and Taylor, Robert T.: Aerodynamic Characteristics of a Flexible-Canopy Paraglider Model at a Mach Number of 4.5 for Angles of Attack to 360° and Sideslip Angles From 0° to 90°. NASA TN D-1776, 1963.

6. Burk, Sanger M., Jr.: Free-Flight Investigation of the Deployment, Dynamic Stability, and Control Characteristics of a 1/12-Scale Dynamic Radio-Controlled Model of a Large Booster and Parawing. NASA TN D-1932, 1963.

7. Sleeman, William C., Jr.: Low-Speed Investigation of Cable Tension and Aerodynamic Characteristics of a Parawing and Spacecraft Combination. NASA TN D-1937, 1963.

8. Libbey, Charles E.: Free-Flight Investigation of the Deployment of a Parawing Recovery Device for a Radio-Controlled 1/5-Scale Dynamic Model Spacecraft. NASA TN D-2044, 1963.

9. Mechtly, E. A.: The International System of Units – Physical Constants and Conversion Factors. NASA SP-7012, 1964.

10. Hewes, Donald E.: Free-Flight Investigation of Radio-Controlled Models With Parawings. NASA TN D-927, 1961.

11. Croom, Delwin R.; Naeseth, Rodger L.; and Sleeman, William C., Jr.: Effects of Canopy Shape on Low-Speed Aerodynamic Characteristics of a 55° Swept Parawing With Large-Diameter Leading Edges. NASA TN D-2551, 1964.

TABLE I.- MODEL GEOMETRIC CHARACTERISTICS

	1/5-scale model		Full-scale model	
Wing area (flat planform measured to center line of leading edge), S	0.51 m^2	(5.54 ft^2)	12.88 m^2	(138.60 ft^2)
Leading-edge length (measured to intersection of center lines), l_{le}	85.3 cm	(33.6 in.)	426.7 cm	(168.0 in.)
Keel length (measured to intersection of center lines), l_k	85.3 cm	(33.6 in.)	426.7 cm	(168.0 in.)
Vertical boom length (measured from top of payload to keel center line)	73.2 cm	(28.8 in.)	365.8 cm	(144.0 in.)
Span (flat planform), b_o	120.9 cm	(47.6 in.)	603.5 cm	(118.8 in.)
Sweep of leading-edge center line				
Λ_o (flat planform)		45^o		45^o
Λ (projected planform)		55^o		55^o

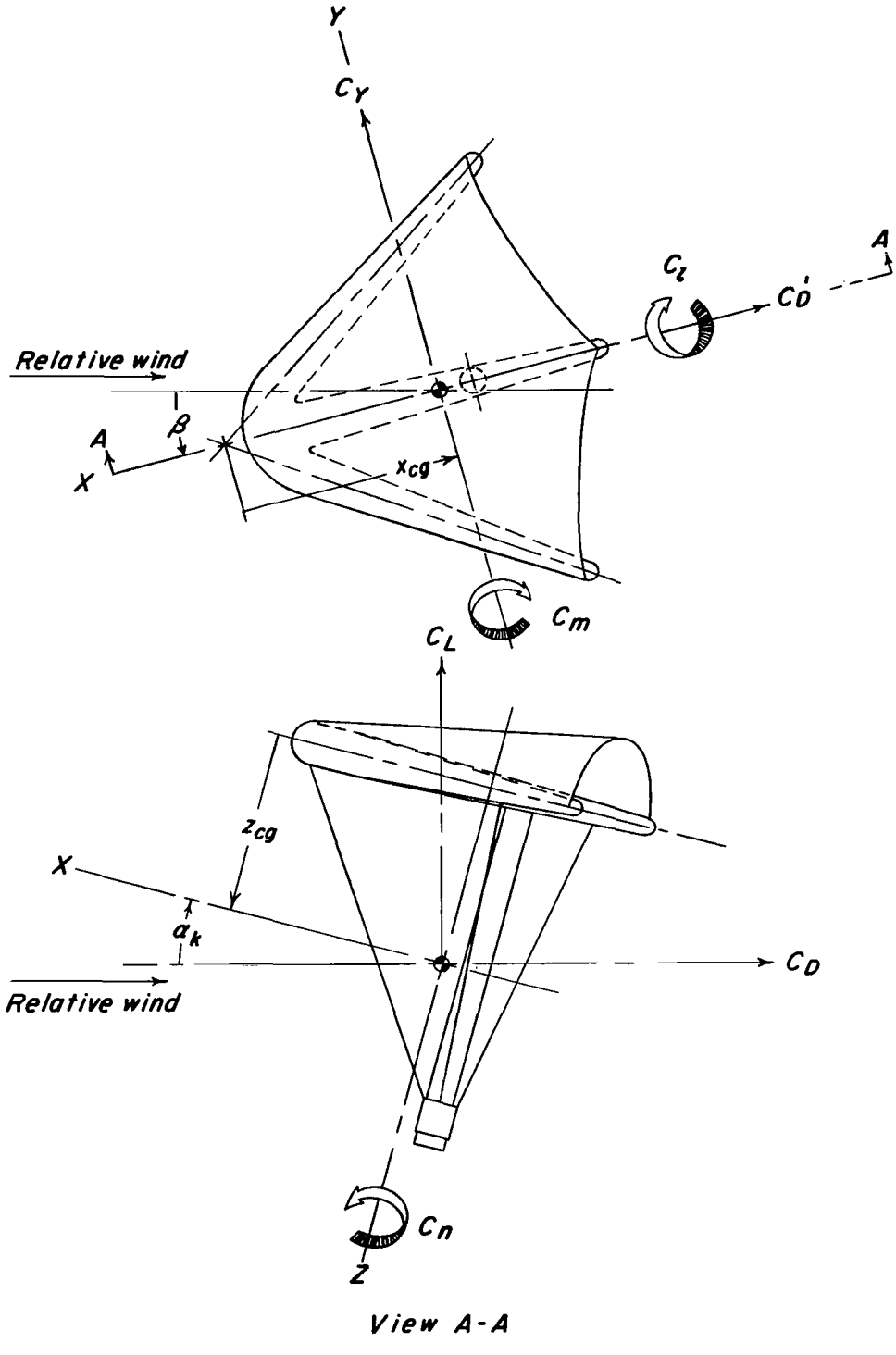

Figure 1.- System of axes used in presentation of data, showing positive direction of forces and moments.

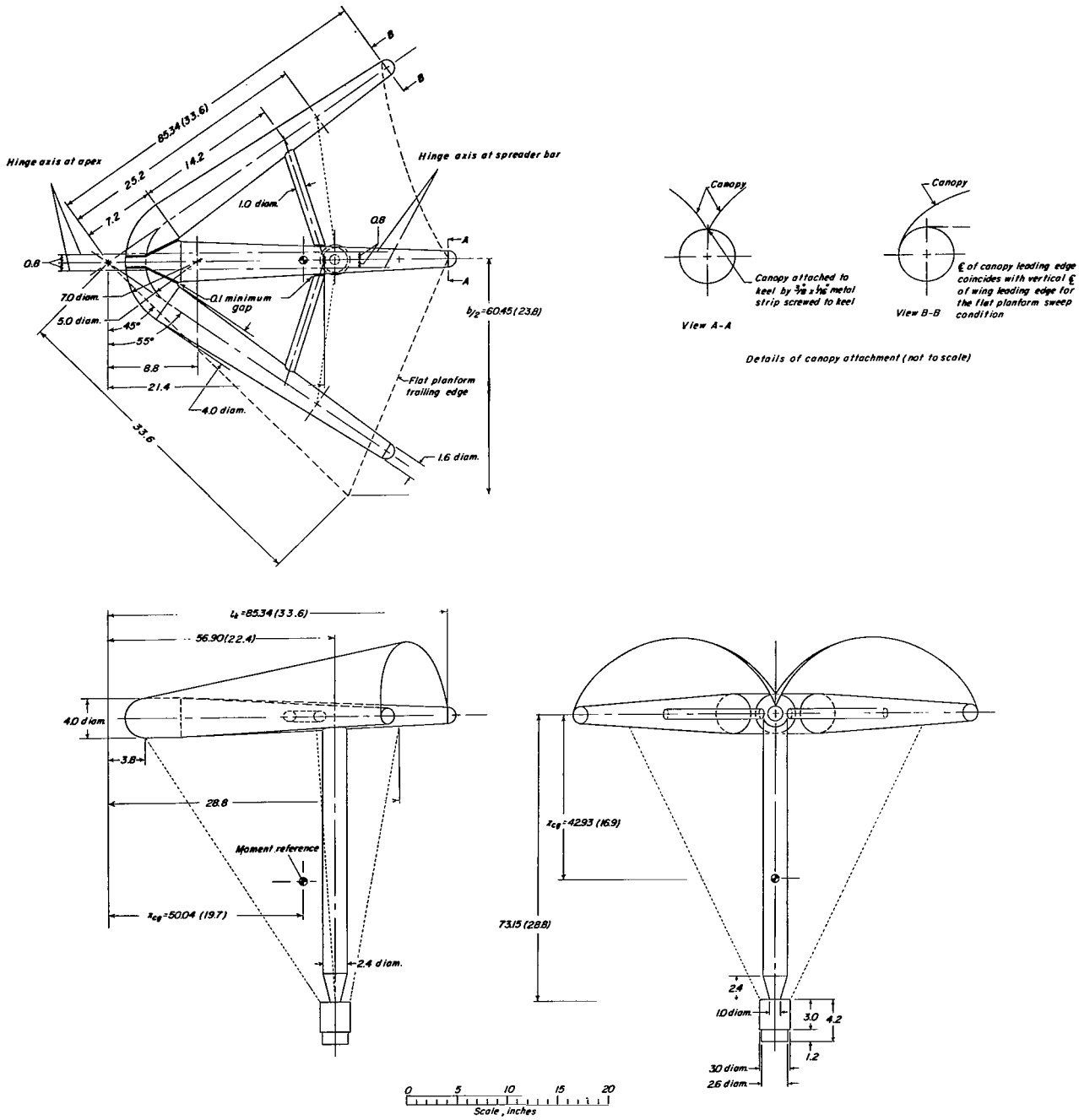

Figure 2.- General arrangement of 1/5-scale complete-model configuration tested in Langley high-speed 7- by 10-foot tunnel. Dimensions are given in inches, except for those converted to the International System of Units. The few representative dimensions converted are given in centimeters with the equivalent value in inches given in parentheses.

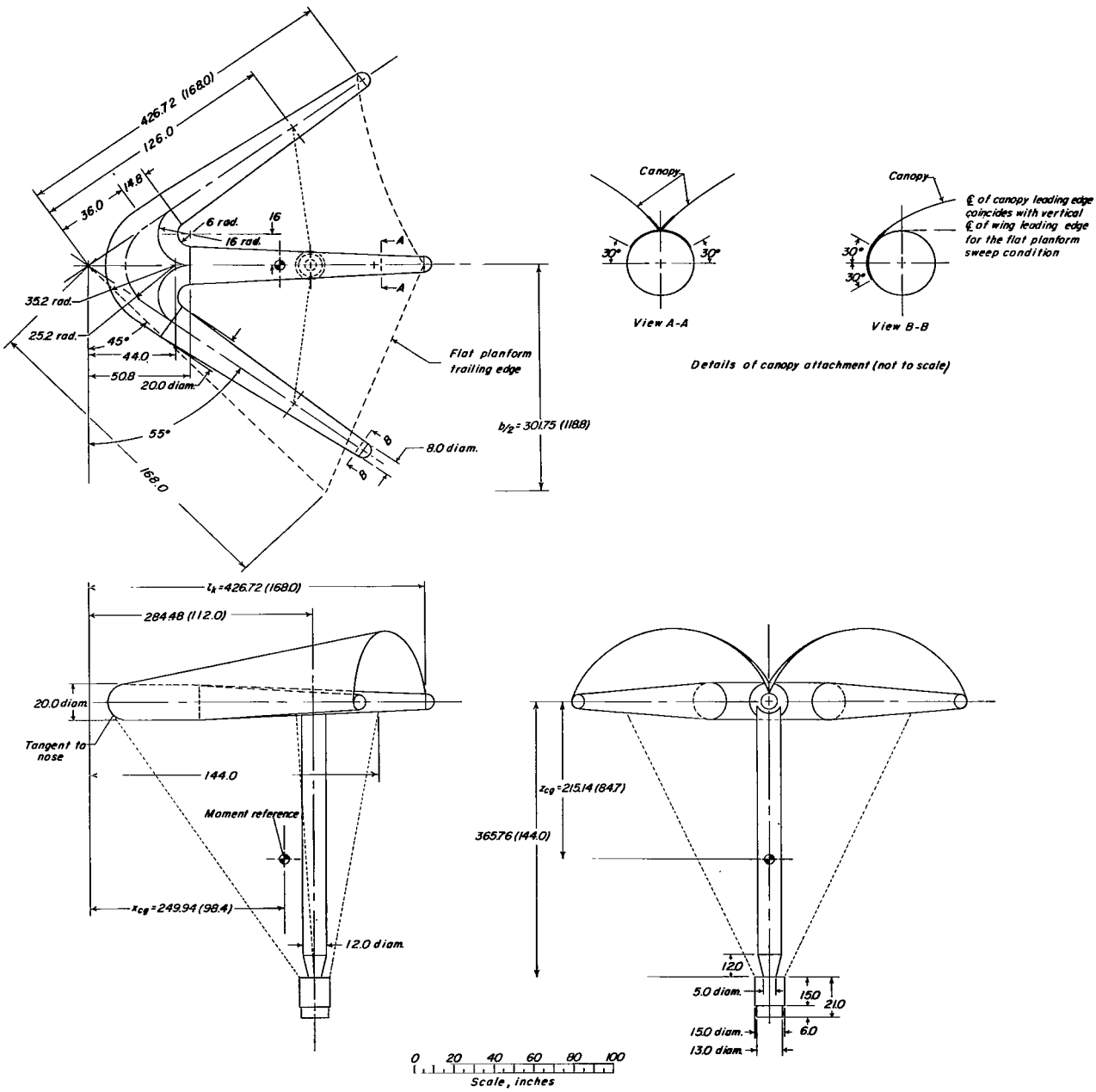

Figure 3.- General arrangement of full-scale complete-model configuration tested in Langley full-scale tunnel. Dimensions are given in inches, except for those converted to the International System of Units. The few representative dimensions converted are given in centimeters with the equivalent value in inches given in parentheses.

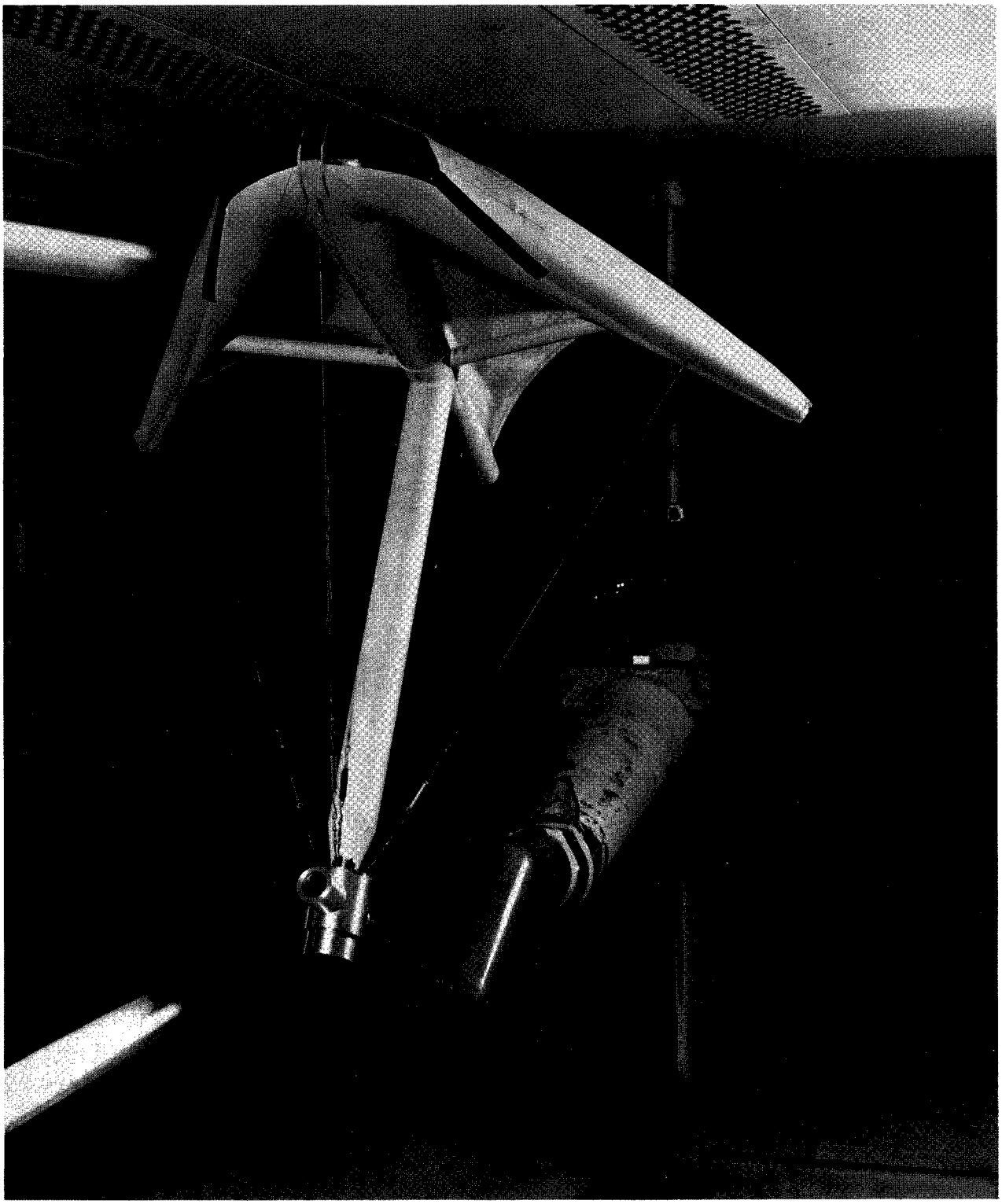

Figure 4.- Photograph of 1/5-scale model in Langley high-speed 7- by 10-foot tunnel. L-62-2879

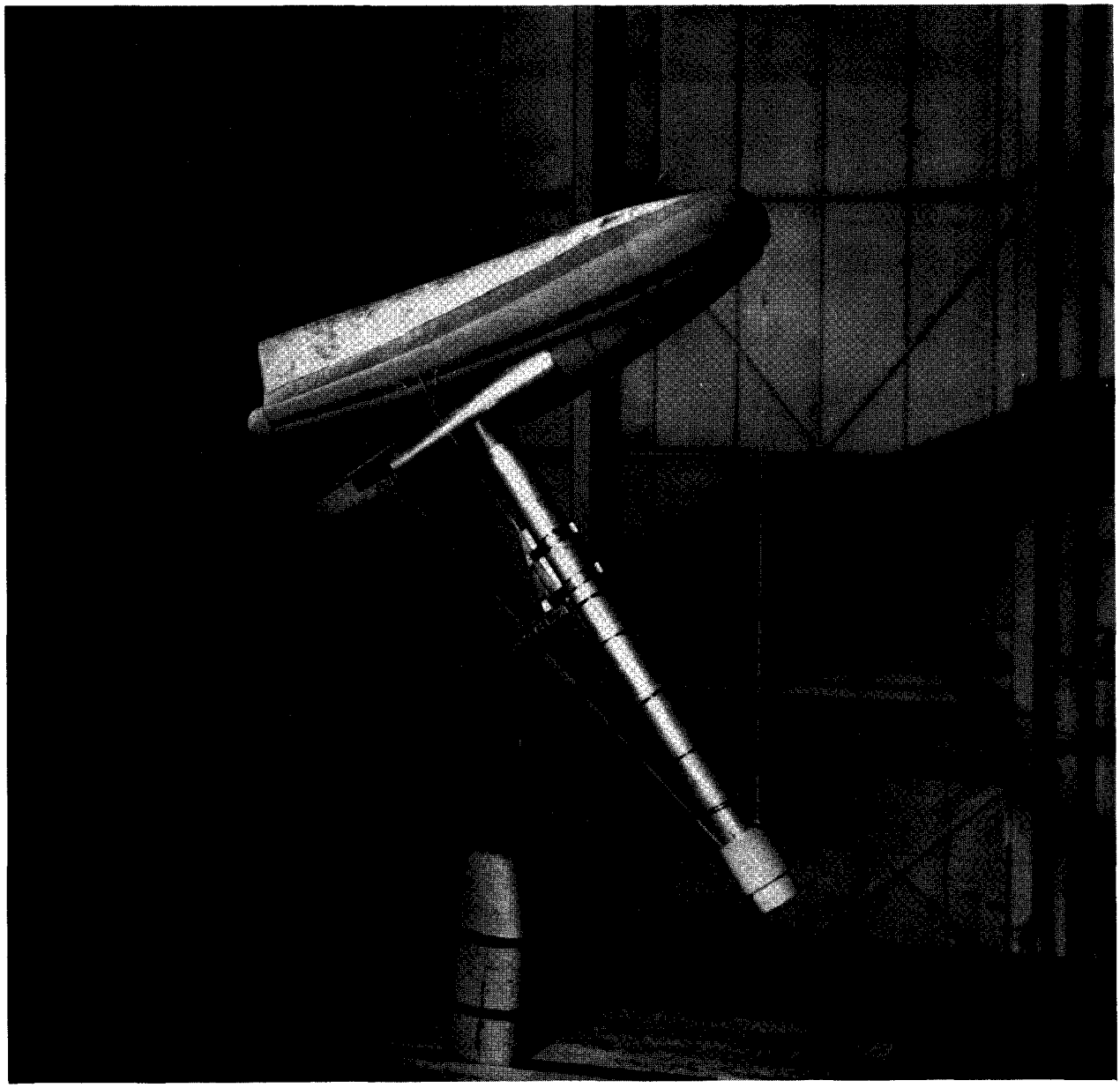

Figure 5.- Photograph of full-scale model in Langley full-scale tunnel. L-62-5998

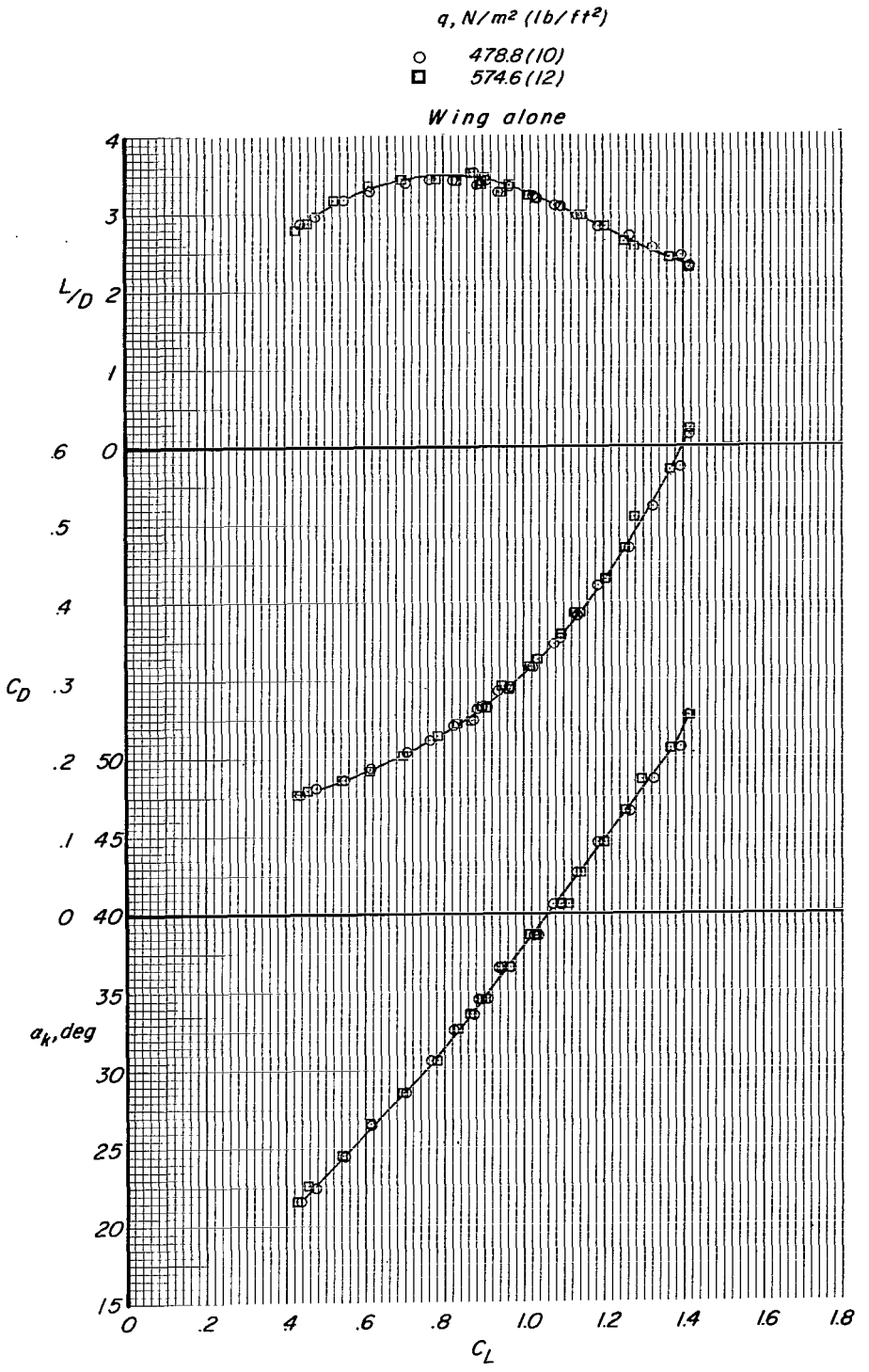

Figure 6.- Static longitudinal aerodynamic characteristics of 1/5-scale wing-alone model configuration tested in Langley high-speed 7- by 10-foot tunnel.

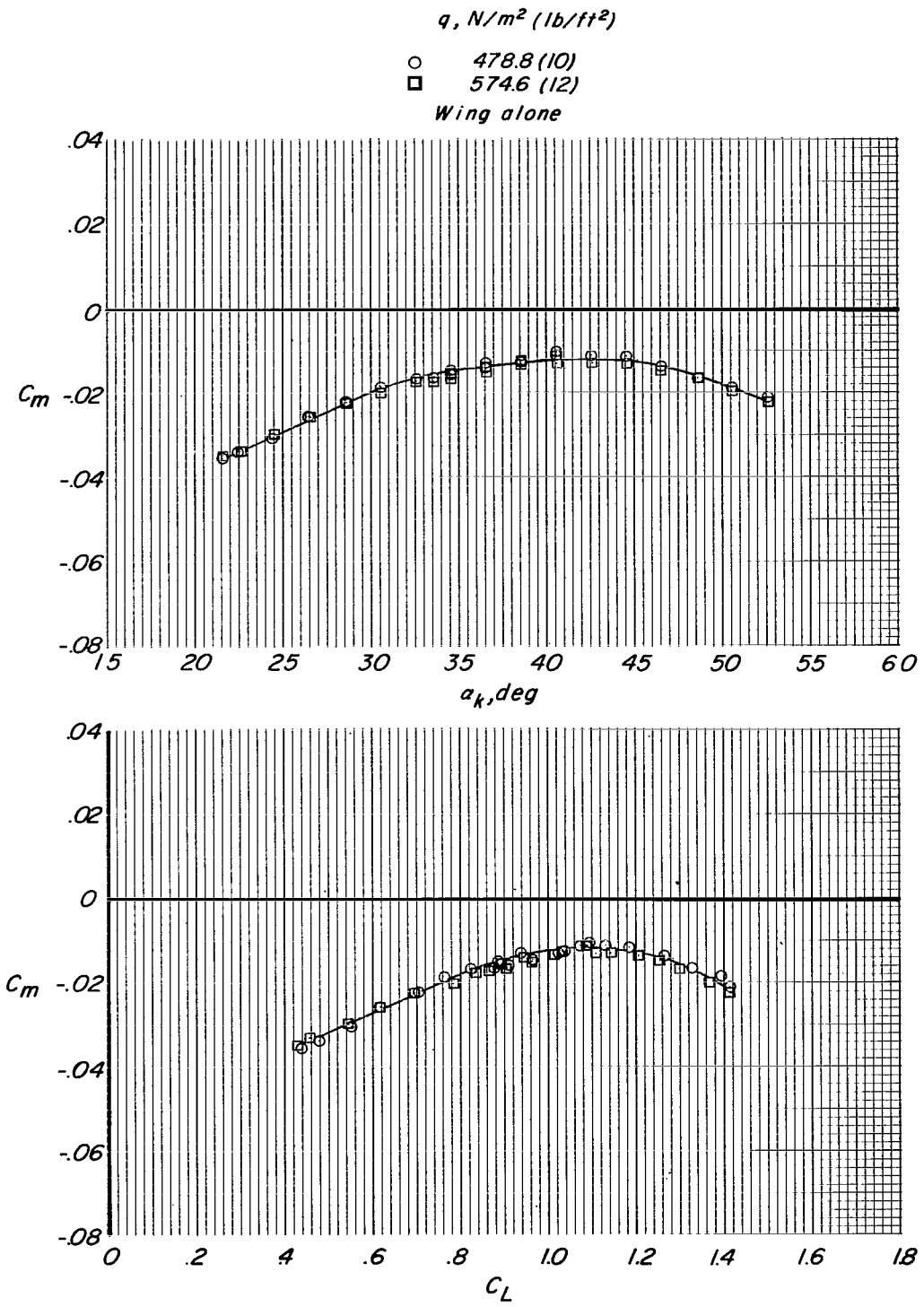

Figure 6.- Continued.

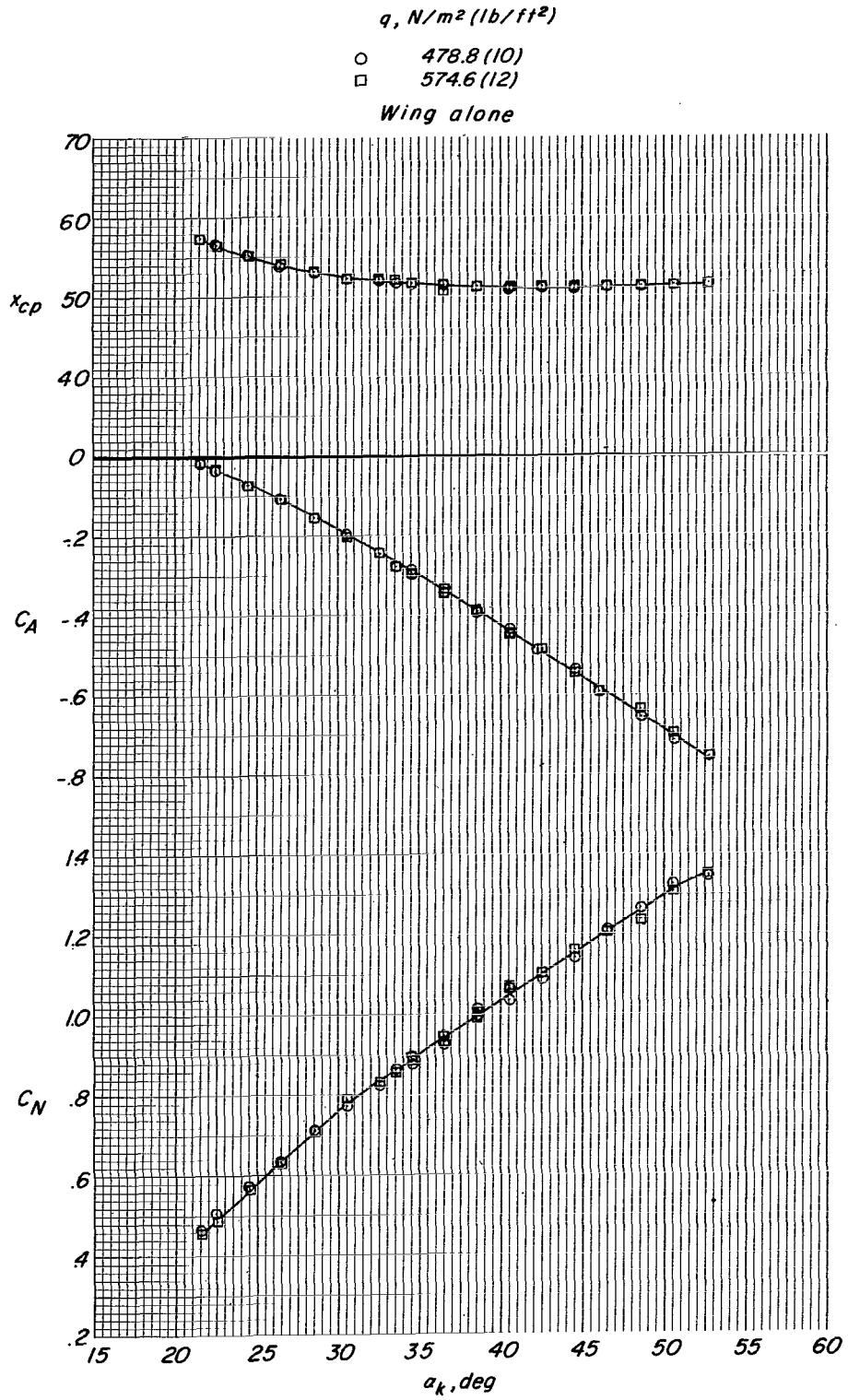

Figure 6.- Concluded.

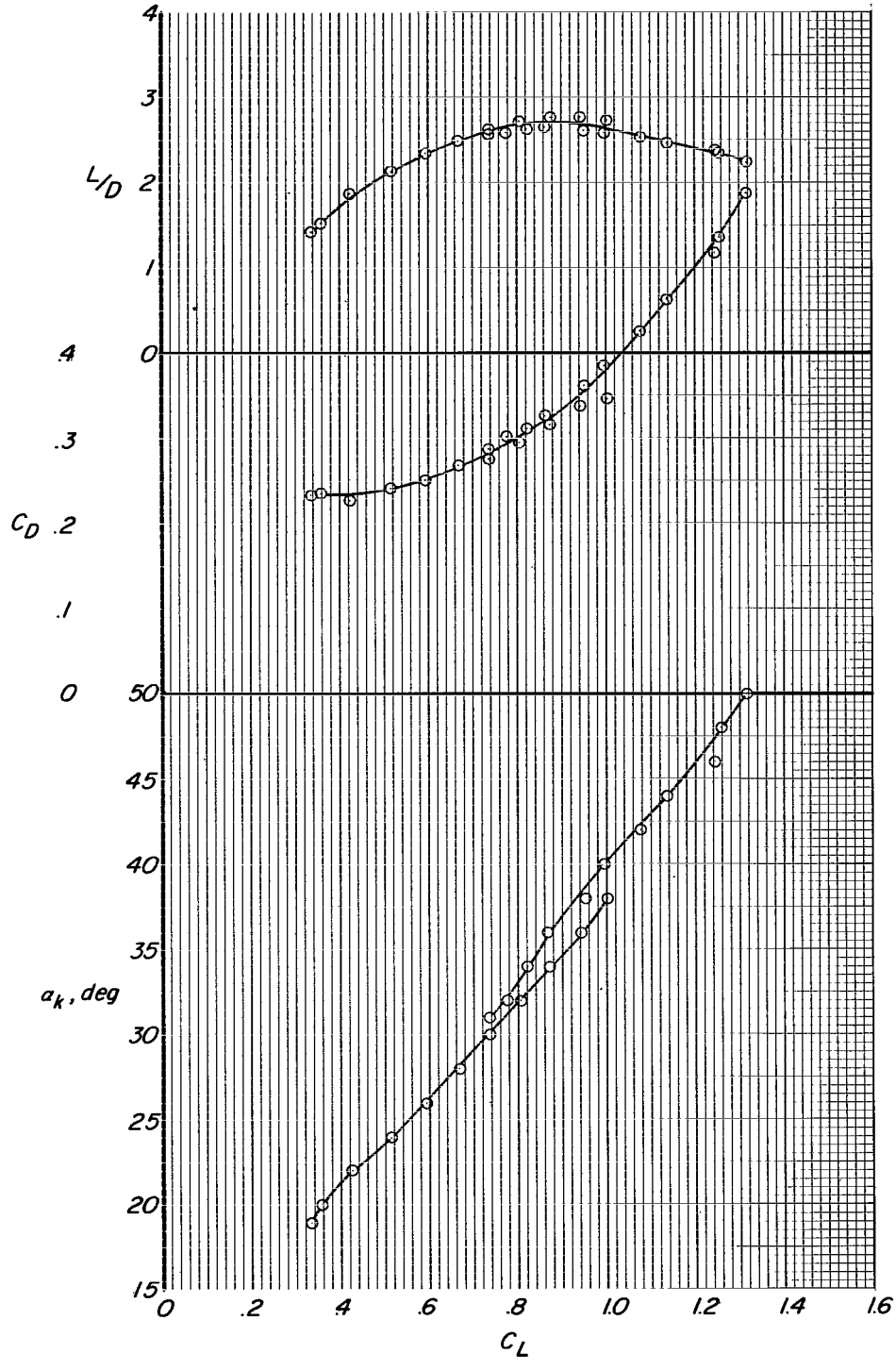

Figure 7.- Static longitudinal aerodynamic characteristics of 1/5-scale complete-model configuration tested in Langley high-speed 7- by 10-foot tunnel. q = 574.6 N/m^2 (12 lb/ft^2).

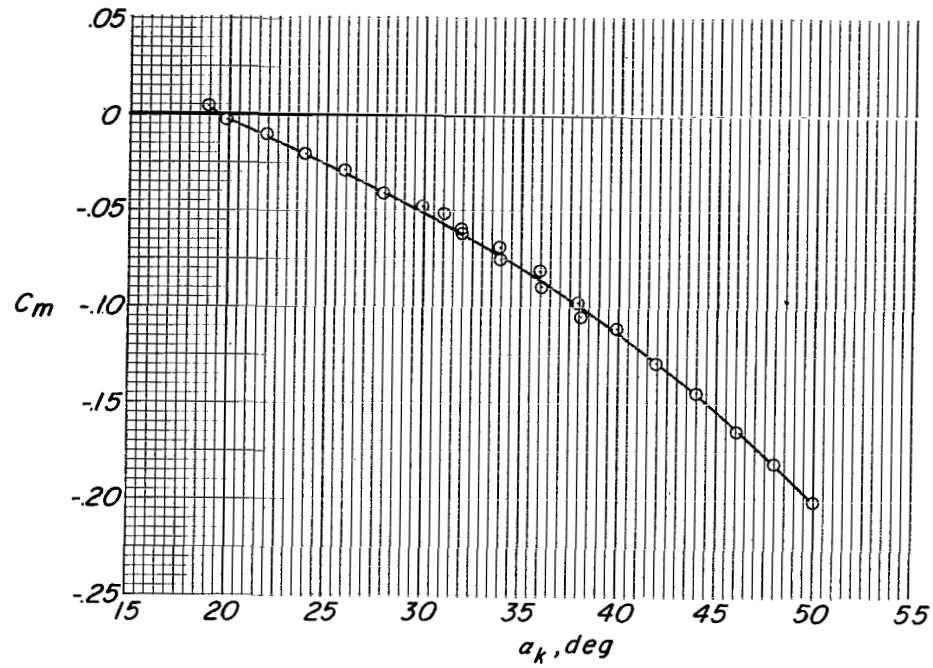

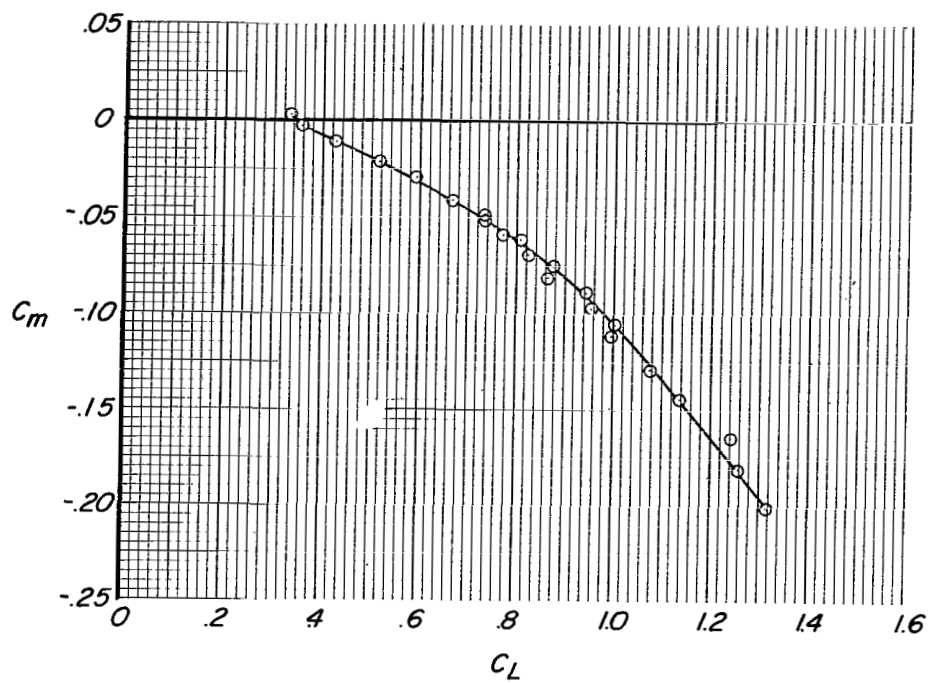

Figure 7.- Concluded.

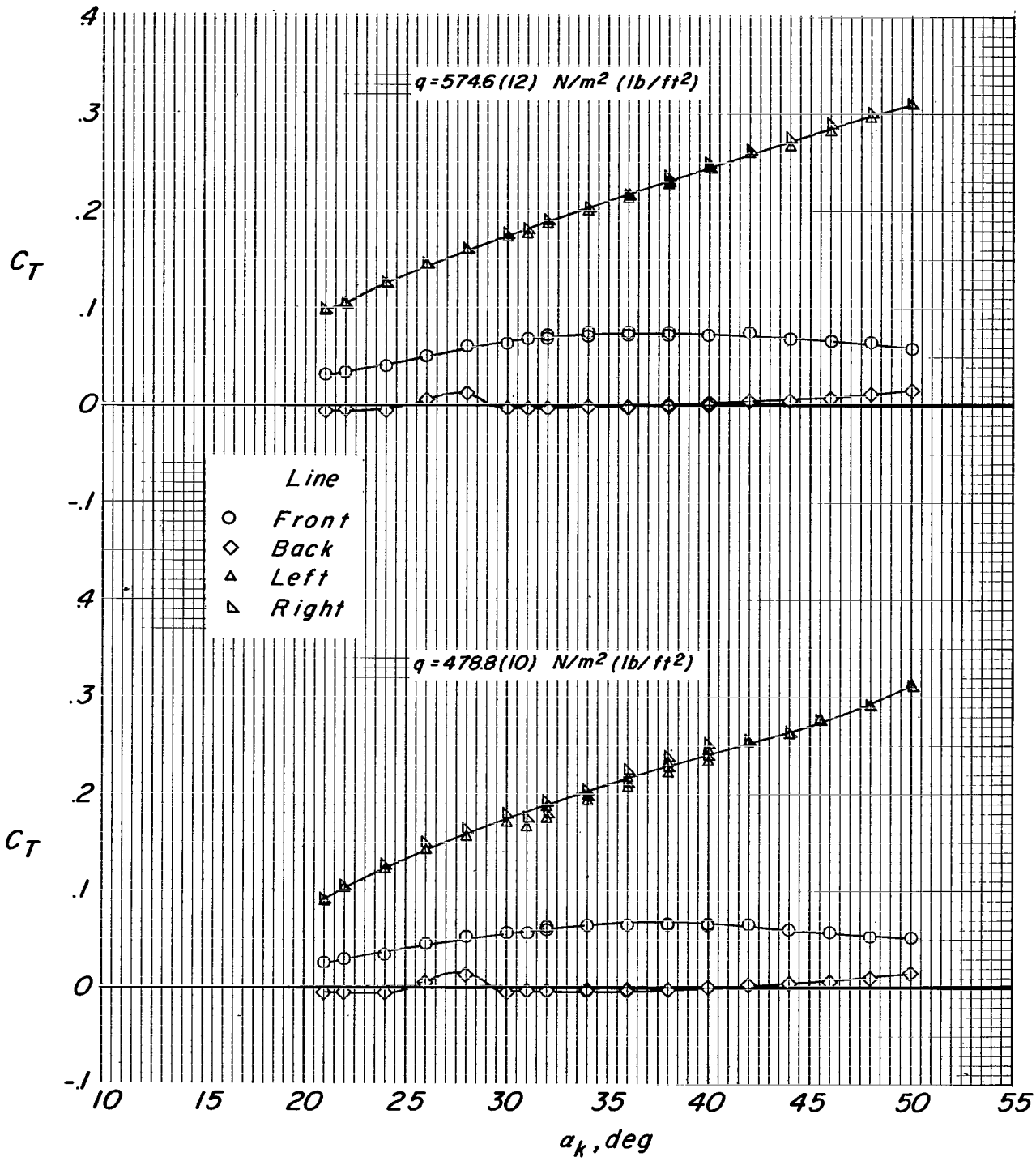

Figure 8.- Effect of angle of attack on cable-tension coefficients of 1/5-scale complete-model configuration tested in Langley high-speed 7- by 10-foot tunnel.

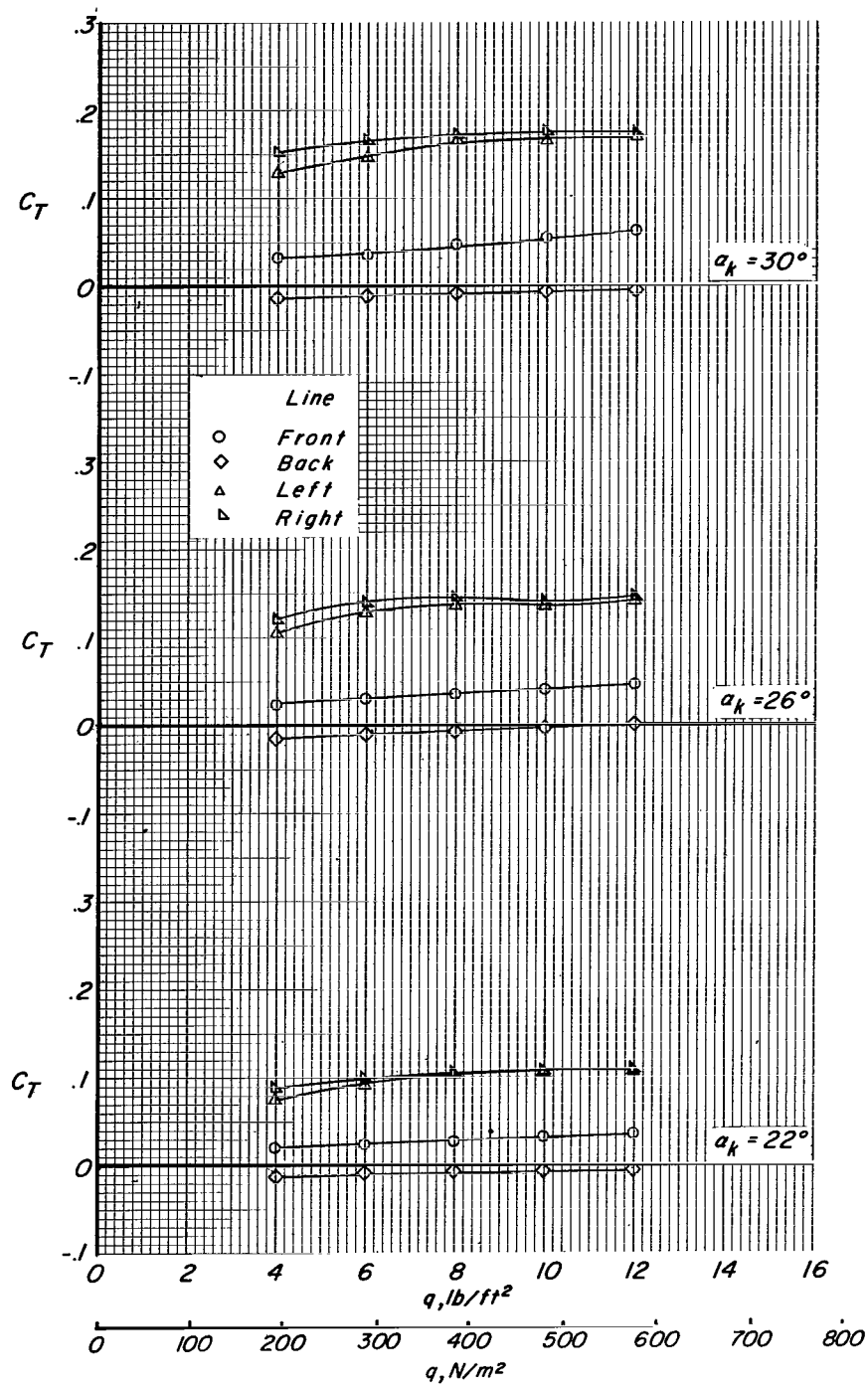

(a) α_k = 22°, 26°, and 30°.

Figure 9.- Effect of dynamic pressure on cable-tension coefficients of 1/5-scale complete-model configuration tested in Langley high-speed 7- by 10-foot tunnel.

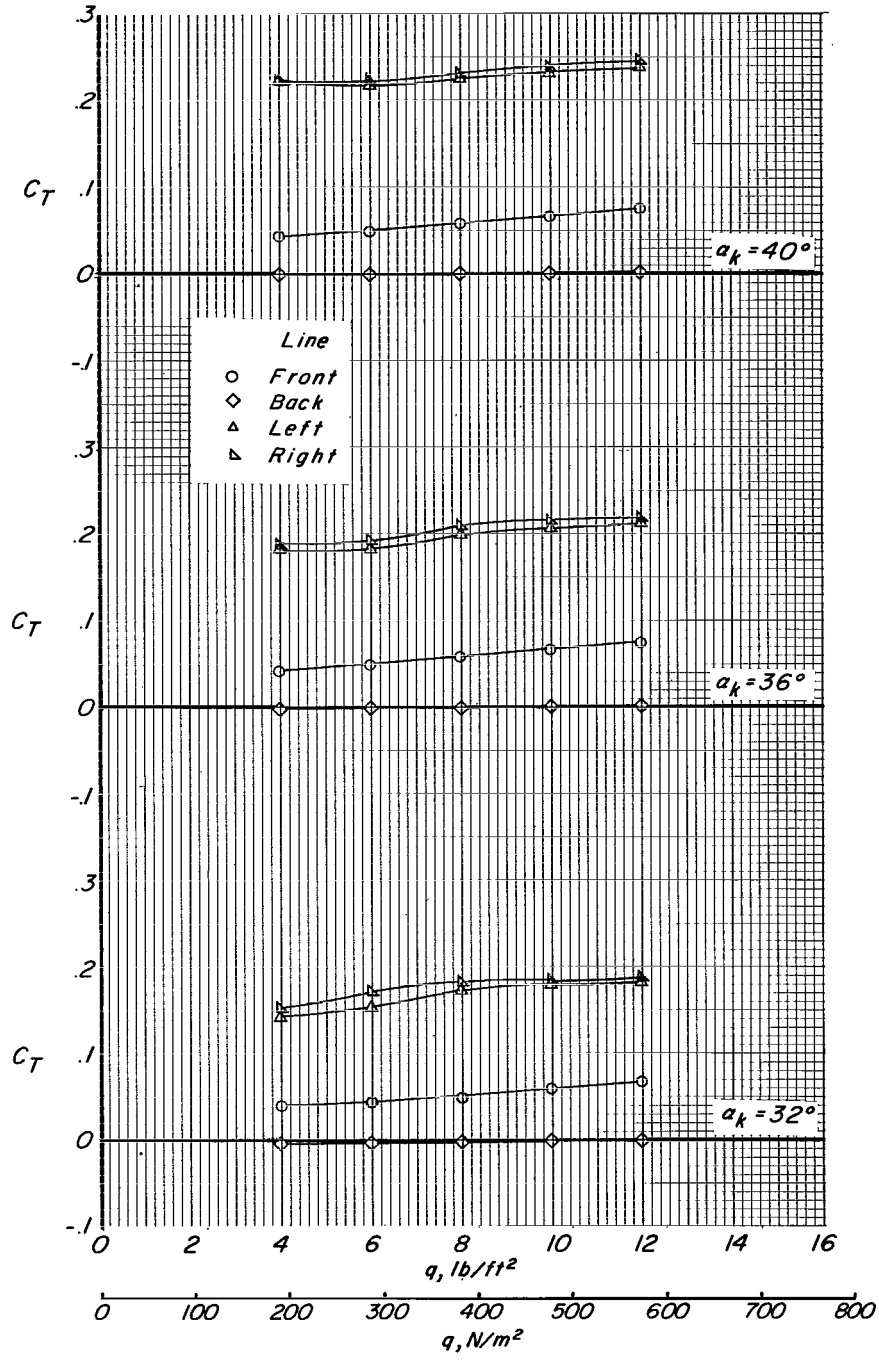

(b) $\alpha_k = 32^0$, 36^0, and 40^0.

Figure 9.- Continued.

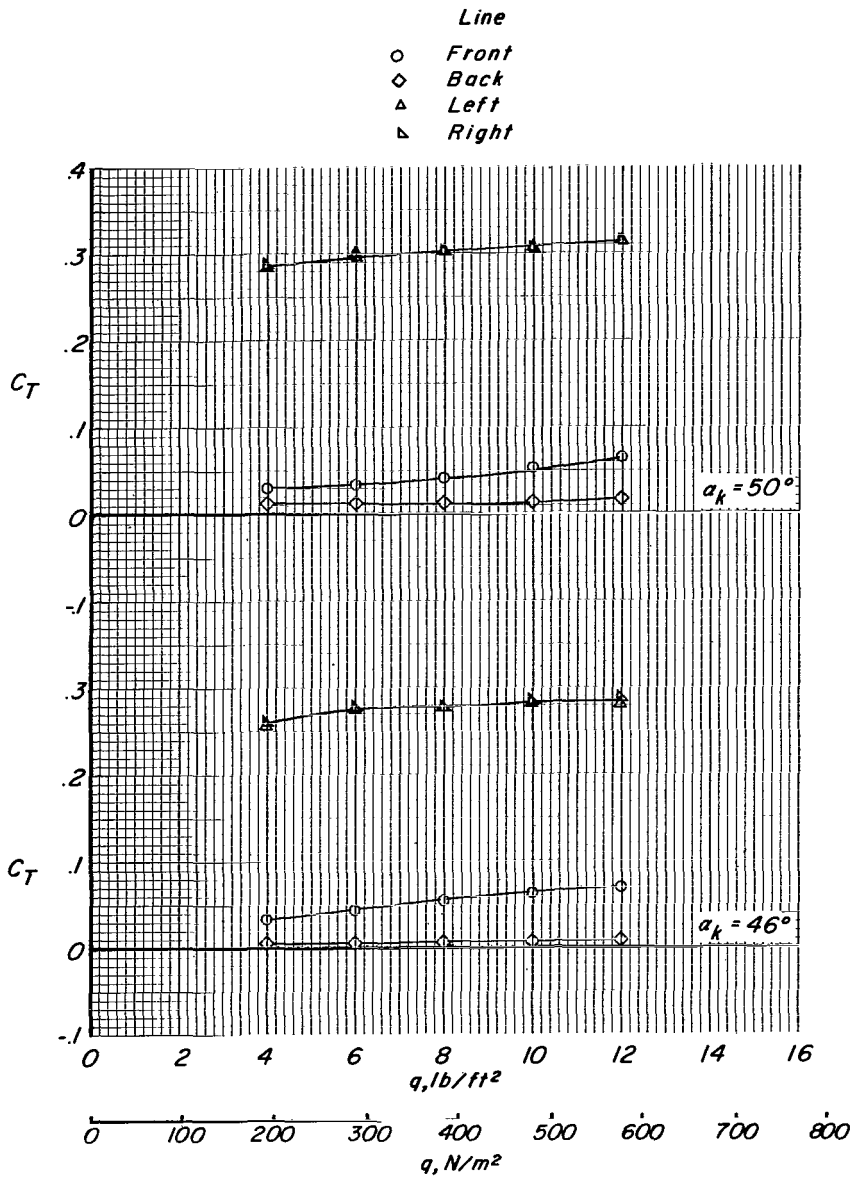

(c) $\alpha_k = 46^0$ and 50^0.

Figure 9.- Concluded.

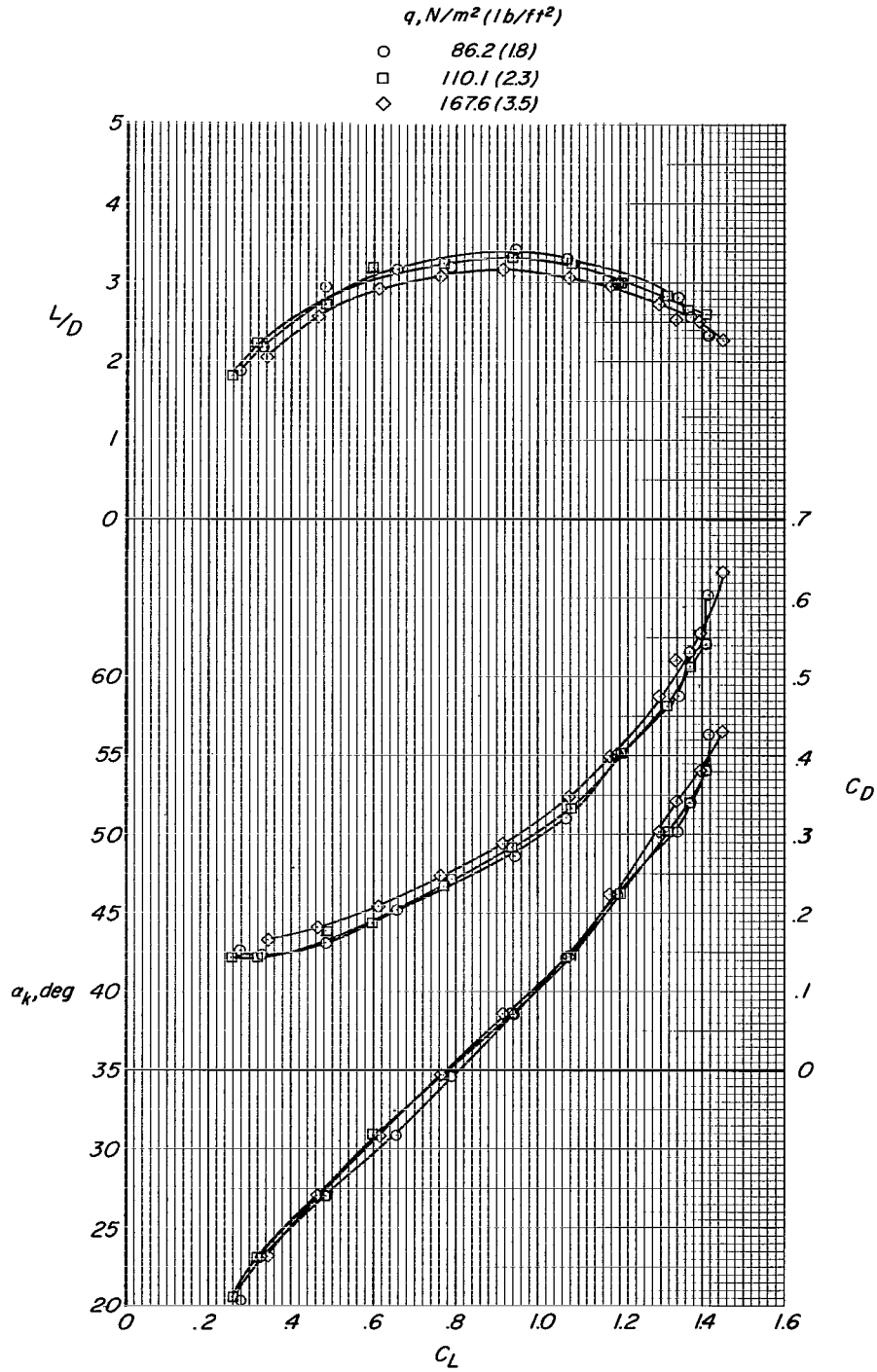

Figure 10.- Static longitudinal aerodynamic characteristics of full-scale complete model tested in Langley full-scale tunnel. Model had nylon suspension lines at leading edge and steel cables at keel.

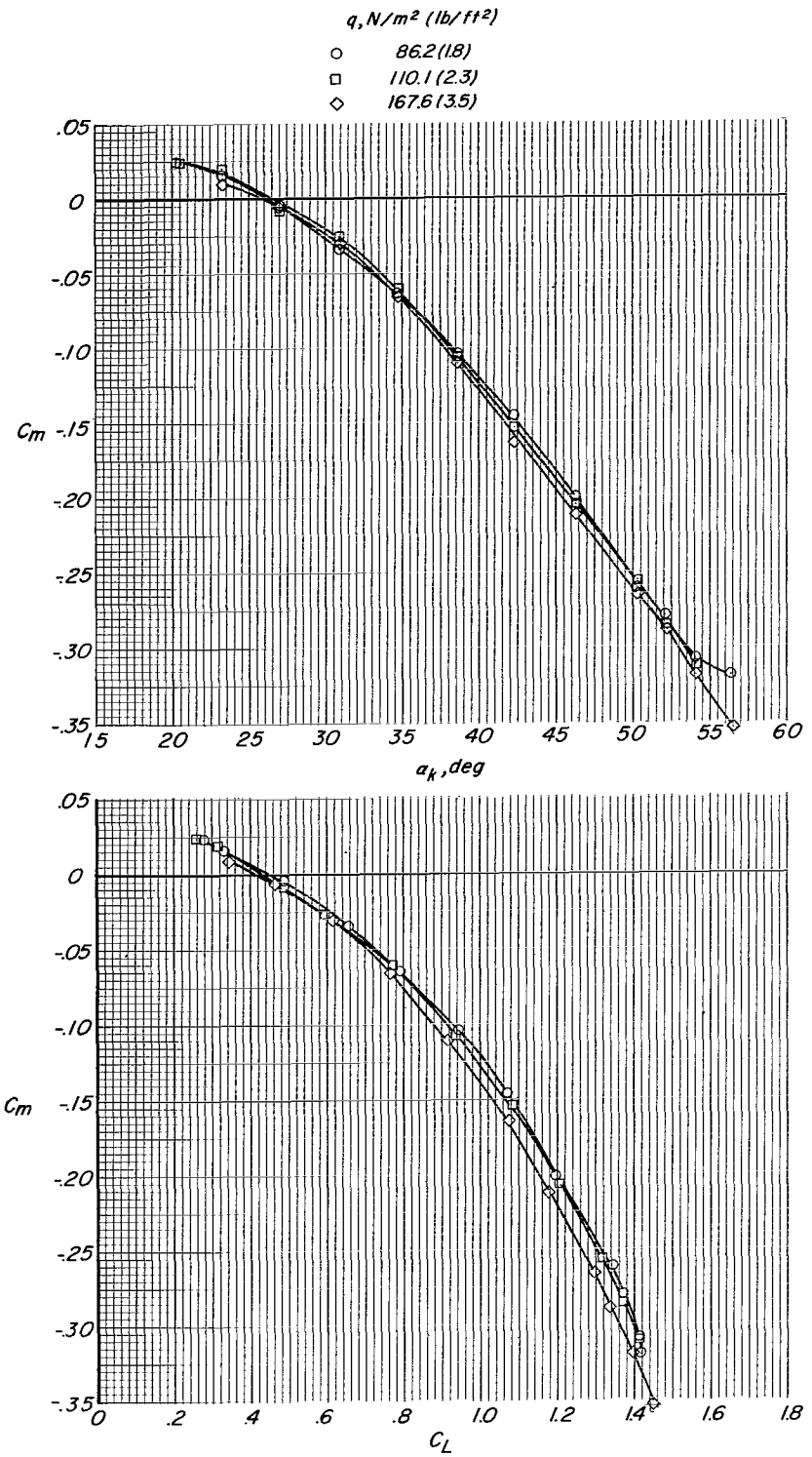

Figure 10.- Concluded.

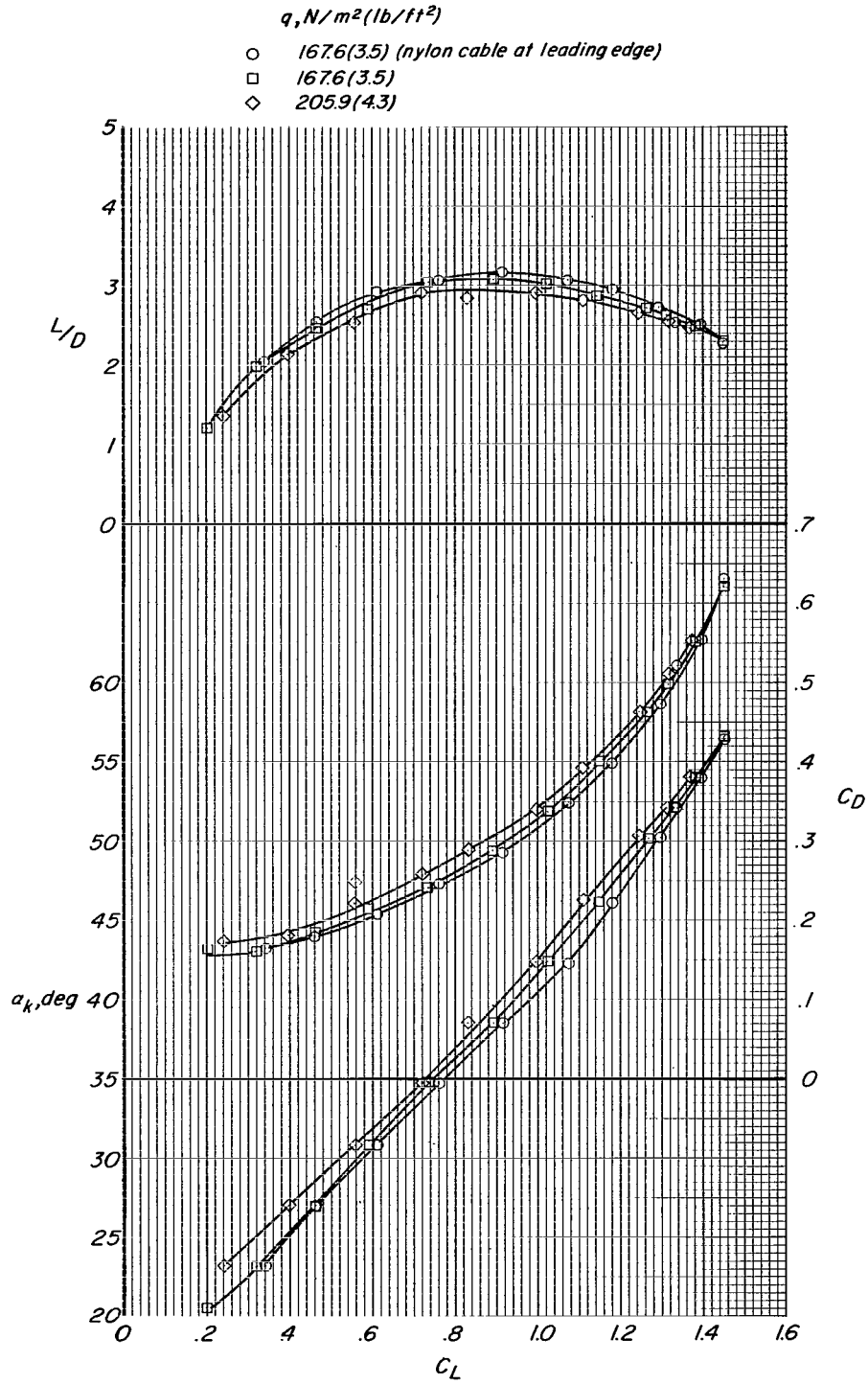

Figure 11.- Static longitudinal aerodynamic characteristics of full-scale complete model tested in Langley full-scale tunnel. Model had steel cable suspension lines at leading edge and keel except as noted.

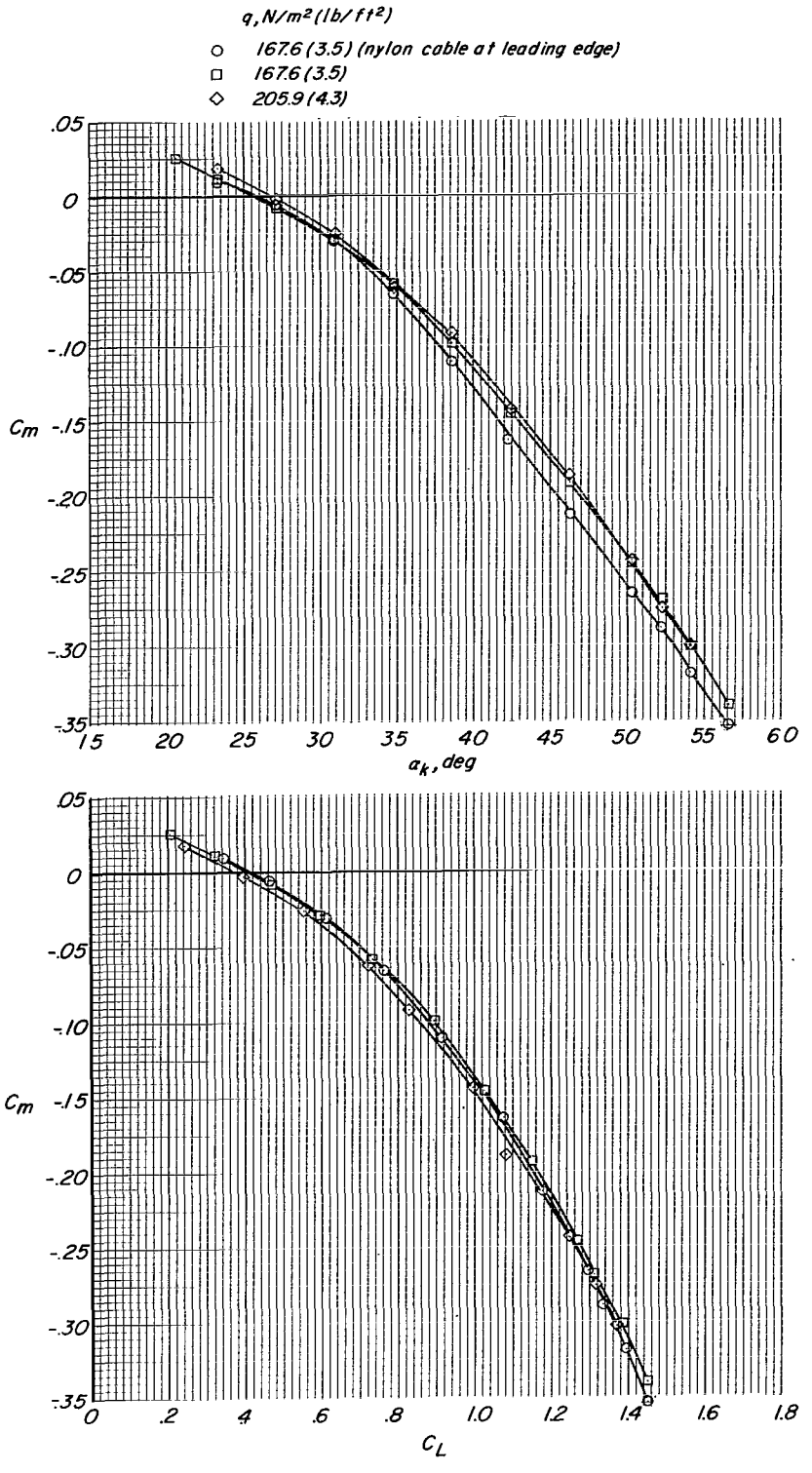

Figure 11.- Concluded.

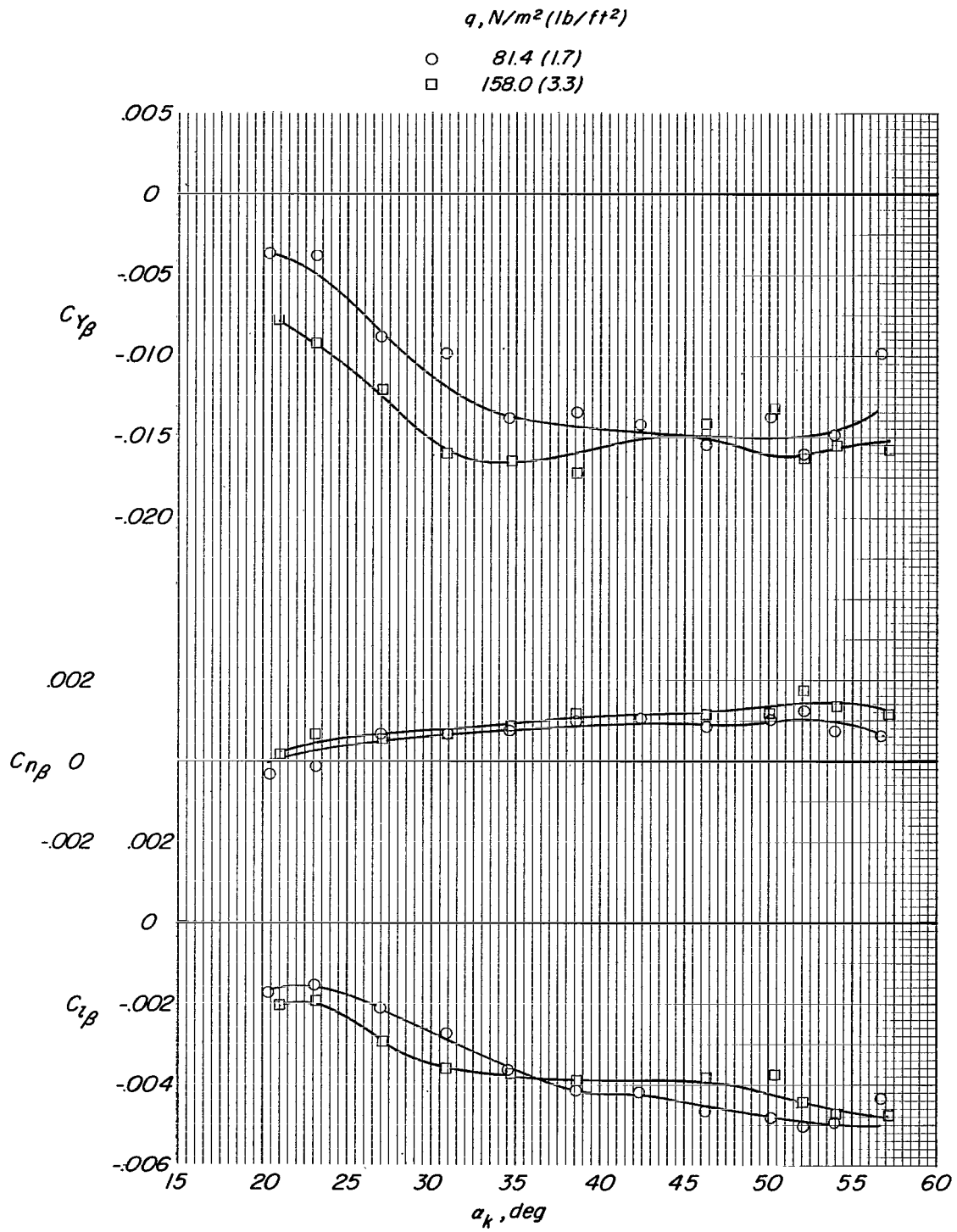

Figure 12.- Static lateral aerodynamic characteristics of full-scale complete model tested in Langley full-scale tunnel. Model had steel cable suspension lines at leading edge and keel.

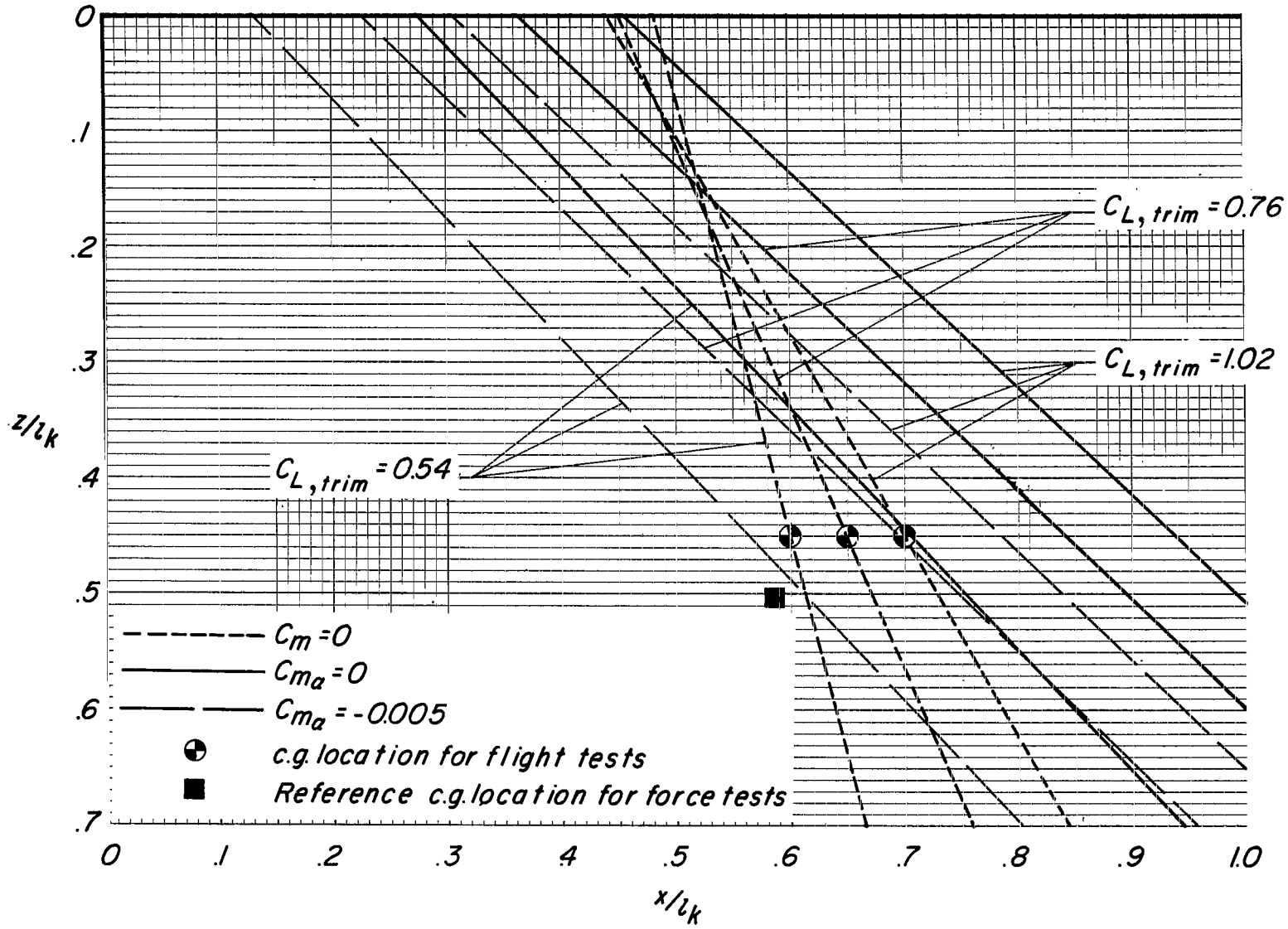

Figure 13.- Effect of center-of-gravity location on trimmed-lift coefficient and static longitudinal stability for full-scale complete model.

A motion-picture film supplement L-906 is available on loan. Requests will be filled in the order received. You will be notified of the approximate date scheduled.

The film (16 mm, 9 min, color, silent) shows steady-state glides and recoveries from unusual attitudes.

Requests for the film should be addressed to:

Chief, Photographic Division
NASA Langley Research Center
Langley Station
Hampton, Va. 23365

CUT

Date _____

Please send, on loan, copy of film supplement L-906 to TN D-3442

_____

Name of organization

_____

Street number

_____

City and State Zip code

Attention: Mr. _____

Title _____

"The aeronautical and space activities of the United States shall be conducted so as to contribute . . . to the expansion of human knowledge of phenomena in the atmosphere and space. The Administration shall provide for the widest practicable and appropriate dissemination of information concerning its activities and the results thereof."

—NATIONAL AERONAUTICS AND SPACE ACT OF 1958

NASA SCIENTIFIC AND TECHNICAL PUBLICATIONS

TECHNICAL REPORTS: Scientific and technical information considered important, complete, and a lasting contribution to existing knowledge.

TECHNICAL NOTES: Information less broad in scope but nevertheless of importance as a contribution to existing knowledge.

TECHNICAL MEMORANDUMS: Information receiving limited distribution because of preliminary data, security classification, or other reasons.

CONTRACTOR REPORTS: Technical information generated in connection with a NASA contract or grant and released under NASA auspices.

TECHNICAL TRANSLATIONS: Information published in a foreign language considered to merit NASA distribution in English.

TECHNICAL REPRINTS: Information derived from NASA activities and initially published in the form of journal articles.

SPECIAL PUBLICATIONS: Information derived from or of value to NASA activities but not necessarily reporting the results of individual NASA-programmed scientific efforts. Publications include conference proceedings, monographs, data compilations, handbooks, sourcebooks, and special bibliographies.

Details on the availability of these publications may be obtained from:

SCIENTIFIC AND TECHNICAL INFORMATION DIVISION

NATIONAL AERONAUTICS AND SPACE ADMINISTRATION

Washington, D.C. 20546